Ruthenium(II) Arene Complexes Containing Benzhydrazone Ligands: Synthesis, Structure and Antiproliferative Activity

Journal:	*Inorganic Chemistry Frontiers*
Manuscript ID	QI-RES-06-2016-000197.R1
Article Type:	Research article
Date Submitted by the Author:	04-Aug-2016
Complete List of Authors:	Mohamed Kasim, Mohamed Subarkhan; Bharathidasan University, School of Chemistry Rengan, Ramesh; Bharathidasan University, School of Chemistry;

Ruthenium(II) Arene Complexes Containing Benzhydrazone Ligands: Synthesis, Structure and Antiproliferative Activity

Mohamed Kasim Mohamed Subarkhan[†] and Rengan Ramesh,*[,†]

[†]School of Chemistry, Bharathidasan University, Tiruchirappalli 620 024, Tamil Nadu, India.

Abstract

Suitable method of synthesis of ruthenium(II) arene benzhydrazone complexes (**1**-**6**) of the general formula [(η^6-arene)Ru(L)Cl] (arene-benzene or *p*-cymene; L-monobasic bidentate substituted 9-anthraldehyde benzhydrazone derivatives) has been described. The composition of the complexes has been established by elemental analysis, IR, UV-vis, emission, NMR and ESI-MS spectral methods. The solid state molecular structure of representative complex was determined by a single-crystal X-ray diffraction study and it indicates the presence of pseudo octahedral (piano stool) geometry. All the complexes have been thoroughly screened for their cytotoxicity against human cervical cancer cells (HeLa), human breast cancer cell line (MDA-MB-231) and human liver carcinoma cells (Hep G2) under *In Vitro* conditions. Interestingly, the cytotoxic activity of the complex **6** is much more potent than cis-platin with low IC_{50} values against all the cancer cell lines tested. Further, the results of AO-EB, Hoechst 33258 and flow cytometry analysis reveal that these complexes induce cell death only through apoptosis. The comet assay has been employed to determine the extent of DNA fragmentation in cancer cells. A hemolysis assay with human erythrocytes demonstrates good blood biocompatibility of all the ruthenium(II) arene benzhydrazone complexes. These results highlight the strong promise to develop highly active ruthenium complexes as anticancer agent.

Introduction

Transition metal complexes remain an important resource for the generation of chemical diversity in the search for novel therapeutic and diagnostic agents, especially in the field of anticancer drug development.[1] Cisplatin represents one of the most active and clinically useful agents used in the treatment of cancer, achieving cures in testicular cancer and high response rates in ovarian and small cell lung cancer.[2] Evidence from both pre-clinical studies and clinical investigations has strongly concerned DNA as the biologic target for cisplatin through the formation of irreversible adducts via the process of ligand exchange. However, in common with many other cytotoxic drugs, cisplatin induces normal tissue

toxicity, particularly to the kidney, and the development of acquired drug resistance can occur in initially responsive disease types.[3] Hence, there is a need for new approaches that are purposefully planned to circumvent these drawbacks. In this regard, ruthenium is considered as a promising metal center for new anticancer agents, with NAMI-A[4] (imidazolium trans-[tetrachloro-dimethylsulfoxide) imidazole ruthenium(III) and KP1019[5] (indazolium trans-[tetrachlorobis(1H-indazole) ruthenium(III) as the most promising ruthenium complexes reaching clinical trials.[6] However, more recently organometallic Ru arene complexes have attracted increasing attention. which is effective against resistant tumors, completed phase I and II clinical trials. RAPTA[7] and RAED[8] compounds are the most intensively investigated organoruthenium complexes and have shown promise in drug development.

In this context, recently, attention has been focused on organometallic Ru(II)-arene complexes are also emerged as an approach to shows potential Ru-based therapeutic agents. Thus, Sadler et al. found that the Ru(II)-arene-en (en, ethylenediamine) complex exhibits efficient cytotoxic activity and also shows activity against cisplatin-resistant cell lines.[9] Adriana Grozav *et al* have described the hydrazinyl-thiazolo arene ruthenium complexes with antiproliferative activity on three tumor cell lines (HeLa, A2780, and A2780cisR) and on a noncancerous cell line (HFL-1) (**A**).[10] Very recently, Sheldrick and coworkers have prepared half-sandwich Ru(II) complexes with methyl-substituted polypyridyl ligands, which strongly bind to DNA and also regulate apoptosis.[11] Synthesis and antiproliferative activity of $Ru^{II}(\eta^6$-arene) compounds carrying bioactive flavonol ligands have been reported by Hartinger et.al (**B**).[12] Wei Su *et al* have described the DNA binding property and anticancer activity of ketone-N^4-substituted thiosemicarbazones and their ruthenium(II) arene complexes.[13] A series of ruthenium(II) arene complexes with the 4-(biphenyl-4-carbonyl)-3-methyl-1-phenyl-5-pyrazolonate ligand, and related 1,3,5-triaza-7-phosphaadamantane (PTA) derivatives, has been reported along with their anticancer activity with low IC_{50} value (**C**).[14] Further, Dyson and his co-workers have reported the synthesis of novel ruthenium half-sandwich complexes containing (N,O)-bound pyrazolone-based β-ketoamine ligands with moderate anticancer activity (**D**) (**Figure 1**).[15] P.J. Sadler and his co-workers have reported ruthenium-arene complexes with curcuminoid analogues possess antiproliferative activity.[16] *In Vitro* and *In Vivo* Evaluation of Water-Soluble Iminophosphorane Ruthenium(II) arene compounds have been reported by Isabel Marzo et al.. Further, these complexes were found to be cytotoxic towards cancerous cell lines (Jurkat, A549, DU-145, MiaPaca2, MDA-MB-231 and HEK-293T) to a comparable extent to cis-platin.[17] Synthesis and antiproliferative activity against

SKOV-3, PC-3, MDA-MB-231 and EC109 cancer cell lines of ruthenium(II) arene N-heterocyclic carbene complexes have been described.[18]

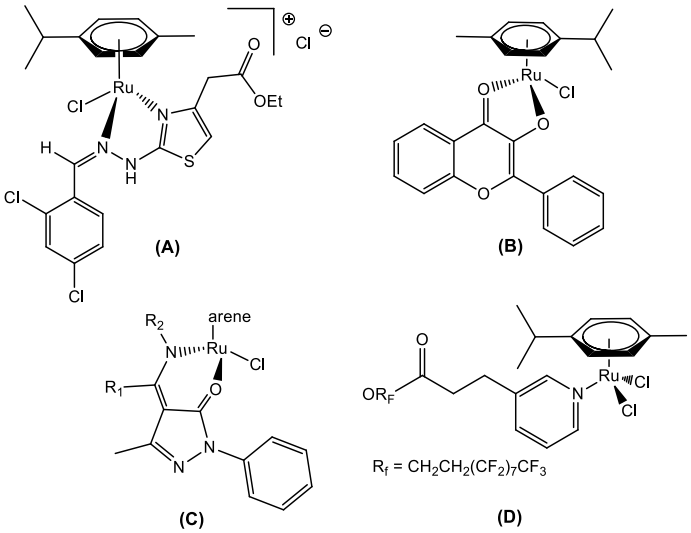

Figure 1. Recently reported ruthenium(II) arene anticancer drugs.

Anthracene and their derivatives are one of the most important classes of ligands with high intrinsic fluorescence and they have been investigated as promising chemotherapeutic agents.[19] Anthracene itself has been reported to be effective against psoriasis. Antitumor activities of anthracyclines can be attributed to their significant inhibitions on the topoisomerase II activity and DNA damage. Bisantrene, as a newly developed anthracycline derivative via organic synthesis for cancer treatment.[20] In this background, we have focused on organic compounds, used as biologically active ligands are derived from pharmacophore anthraquinone compounds with hydrazone moieties due to the identification of several hydrazone lead compounds showing antiproliferative activity[21] and antitumor activity.[22] It has been found from the literature that only a few reports are available on synthesis, characterisation and cytotoxicity of ruthenium(II) complexes containing hydrazone ligands.[23] Nevertheless, it should be pointed out that, as far as we know, the biological properties of arene ruthenium complexes bearing aroylhydrazones have not been explored until now. Therefore, in this study, we have combined ruthenium unit with anthraquinone moiety and benzhydrazone ligand to generate a series of organometallic compounds with significant anticancer activity, taking advantage of the synthetic versatility of hydrazone derivatives and the promising biological activity (**Figure 2**).

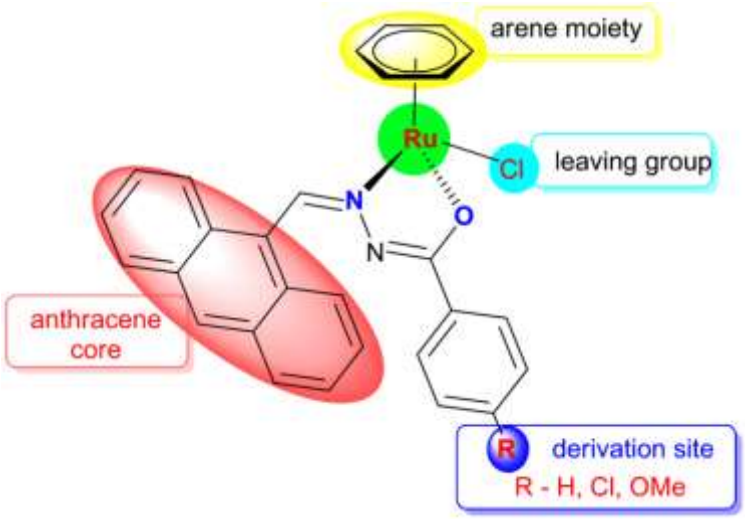

Figure 2. Design of Ru(II) arene 9-Anthraldehyde benzhydrazone complexes

In the present study, the synthesis and characterization of Ru(II) arene complexes containing bidentate 9-anthraldehyde benzhydrazone ligands and chlorine. All the synthesized complexes have been characterized by elemental analysis, IR, UV-vis and NMR and ESI-MS spectroscopy techniques. The molecular structure of the complex **5** is confirmed through single crystal X-ray diffraction. The *in vitro* cytotoxicity of the complexes **1-6** against HeLa, MDA-MB-231, Hep G2 and NIH 3T3 were screened by MTT assay. The morphological changes were employed using various biochemical apoptosis assays (AO-EB staining, Hoechst staining, flow cytometry technique and comet assay). All the complexes are exhibited negligible red hemoglobin release, implying that it is negligibly toxic or safe to normal cells.

Experimental Section

Methods and Instrumentation

The microanalysis of carbon, hydrogen, nitrogen and sulphur were recorded by an analytical function testing Vario EL III CHNS elemental analyser at the sophisticated Test and Instrumentation Centre (STIC), Cochin University, Kochi. Melting points were recorded with a Boetius micro-heating table and are corrected. FT-IR spectra were recorded in KBr pellets with JASCO 400 plus spectrometer. Electronic spectra in chloroform solution were recorded with a CARY 300 Bio UV- visible Varian spectrometer. Emission intensity measurements were carried out by using a Jasco FP-6500 Spectrofluorimeter with 5 nm exit slit. ^{1}H NMR spectra were recorded on a Bruker 400 MHz instrument using tetramethylsilane (TMS) as an internal reference. A Micro mass Quattro II triple quadrupole mass spectrometer was employed for electrospray ionization mass spectrometry (ESI-MS).

Materials

The starting materials $[(\eta^6\text{-p-cymene})RuCl_2]_2$ and $(\eta^6\text{-benzene})RuCl_2]_2$ were prepared according to literature methods.[24]

Procedure for the preparation of 9-Anthraldehyde benzhydrazones ligands

A mixture of 4-substituded benzhydrazide (1 mmol) and 9-Anthraldehyde (1 mmol) in ethanol (10 mL) containing a drop of glacial acetic acid was refluxed for 30 min. The separated solid was filtered and dried in air. Ligands were further purified by recrystallisation from methanol.[25] Yield**:** 67-92%.

Procedure for the synthesis of ruthenium(II) arene benzhydrazone complexes

A mixture containing starting $[(\eta^6\text{-arene})RuCl_2]_2$ (arene=benzene or *p*-cymene) (0.05 mmol), 9-Anthraldehyde benzhydrazone ligand (0.1 mmol) and triethylamine (0.3 mL) in benzene (20 ml) was taken in a clean 50 ml round bottom flask. The resulting mixture was allowed to react with stirring at room temperature for 2 h. A color change of the solution from dark red to orange brown was observed. The solution was concentrated to 2 mL, and hexane was added to initiate precipitation of the complex. The reaction progress was monitored through thin layer chromatography.

$[Ru(\eta^6\text{-}C_6H_6)(Cl)(L1)]$ (1): Brown solid. Yield = 0.160 g (68%); M.p.: 183^0C (with decomposition); Calculated: $C_{28}H_{21}ClN_2ORu$: C, 62.51; H, 3.93; N, 5.21%. Found: C, 62.57; H, 3.94; N, 5.25%. IR (KBr, cm^{-1}):1531 $\nu_{(C=N-N=C)}$, 1486 $\nu_{(N=C-O)}$, 1375 $\nu_{(C-O)}$. UV–Vis (CH_3CN, λ_{max}/nm (ε_{max}/dm^3 mol^{-1} cm^{-1}): 410 (1143), 278 (6371), 232 (14,757). ^{1}H NMR (400 MHz, $CDCl_3$) (δ ppm): 9.71 (s, 1H, HC=N), 7.43–8.54 (m, 14H, aromatic), 4.64 (s, 6H, CH-benzene). ESI-MS: displays a peak at m/z 502.46 $(M - Cl)^+$ (calcd m/z 502.48).

$[Ru(\eta^6\text{-}C_6H_6)(Cl)(L2)]$ (2): Brown solid. Yield = 0.0933 g (69%); M.p.: 196^0C (with decomposition); Calculated: $C_{28}H_{20}Cl_2N_2ORu$: C, 58.75; H, 3.52; N, 4.89 %. Found: C, 58.73; H, 3.51; N, 4.86 %. IR (KBr, cm^{-1}): 1533 $\nu_{(C=N-N=C)}$, 1471 $\nu_{(N=C-O)}$, 1383 $\nu_{(C-O)}$. UV–Vis (CH_3CN, λ_{max}/nm (ε_{max}/dm^3 mol^{-1} cm^{-1}): 419 (1044), 267 (4977), 236 (10,051). ^{1}H NMR (400 MHz, $CDCl_3$) (δ ppm): 9.64 (s, 1H, HC=N), 7.34–8.68 (m, 13H, aromatic), 4.63 (s, 6H, CH-benzene). ESI-MS: displays a peak at m/z 537.02 $(M - Cl)^+$ (calcd m/z 536.99).

[Ru(η^6-C_6H_6)(Cl)(L3)] (3): Orange brown solid. Yield = 0.268 g (92%); M.p.: 174^{0}C (with decomposition); Calculated: $C_{29}H_{23}ClN_2O_2Ru$: C, 61.32; H, 4.08; N, 4.93 %. Found: C, 61.34; H, 4.04; N, 4.95 %. IR (KBr, cm^{-1}):1524 $\nu_{(C=N-N=C)}$, 1479 $\nu_{(N=C-O)}$, 1352 $\nu_{(C-O)}$. UV–Vis (CH_3CN, λ_{max}/nm (ε_{max}/dm^3 mol^{-1} cm^{-1}): 421 (1496), 262 (4904), 236 (10,242). ^{1}H NMR (400 MHz, $CDCl_3$) (δ ppm): 9.61 (s, 1H, HC=N), 6.87-8.57 (m, 13H, aromatic), 4.62 (s, 6H, CH-benzene), 3.84 (s, 3H, OCH_3). ESI-MS: displays a peak at m/z 532.58 $(M - Cl)^+$ (calcd m/z 532.50).

[Ru(η^6-p-cymene)(Cl)(L1)] (4): Orange solid. Yield = 0.240 g (80%); M.p.: 189^{0}C (with decomposition); Calculated: $C_{32}H_{31}ClN_2ORu$: C, 64.47; H, 5.24; N, 4.70% Found: C, 64.49; H, 5.26; N, 4.68%. IR (KBr, cm^{-1}):1528 $\nu_{(C=N-N=C)}$, 1486 $\nu_{(N=C-O)}$, 1371 $\nu_{(C-O)}$. UV–Vis (CH_3CN, λ_{max}/nm (ε_{max}/dm^3 mol^{-1} cm^{-1}): 409 (1044), 259 (4941), 229 (11,908). ^{1}H NMR (400 MHz, $CDCl_3$) δ (ppm): 9.62 (s, 1H, HC=N), 7.27–8.55 (m, 14H, aromatic), 5.37 (d, 1H, p-cym-H), 5.02 (d, 1H, p-cym-H), 4.77 (d, 1H, p-cym-H), 4.36 (d, 1H, p-cym-H), 3.11 (m, 1H, p-cym $CH(CH_3)_2$), 2.48 (s, 3H, p-cym CCH_3), 1.41 (d, 3H, p-cym $CH(CH_3)_2$, 1.02 (d, 3H, p-cym $CH(CH_3)_2$. ESI-MS: displays a peak at m/z 559.05 $(M - Cl)^+$ (calcd m/z 559.00).

[Ru(η^6-p-cymene)(Cl)(L2)] (5): Orange solid. Yield = 0.269 g (82%); M.p.: 202^{0}C (with decomposition); Calculated: $C_{32}H_{28}Cl_2N_2ORu$: C, 61.15; H, 4.49; N, 4.46 %. Found: C, 61.13; H, 4.53; N, 4.46%. IR (KBr, cm^{-1}):1538 $\nu_{(C=N-N=C)}$, 1489 $\nu_{(N=C-O)}$, 1369 $\nu_{(C-O)}$. UV–Vis (CH_3CN, λ_{max}/nm (ε_{max}/dm^3 mol^{-1} cm^{-1}): 412 (1237), 267 (6908), 231 (15,482). ^{1}H NMR (400 MHz, $CDCl_3$) δ (ppm): 9.60 (s, 1H, HC=N), 7.49-8.68 (m, 13H, aromatic), 5.35 (d, 1H, p-cym-H), 5.01 (d, 1H, p-cym-H), 5.00 (d, 1H, p-cym-H), 4.36 (d, 1H, p-cym-H), 2.48 (m, 1H, p-cym $CH(CH_3)_2$), 2.18 (s, 3H, p-cym CCH_3), 1.41 (d, 3H, p-cym $CH(CH_3)_2$, 1.00 (d, 3H, p-cym $CH(CH_3)_2$. ESI-MS: displays a peak at m/z 591.75 $(M - HCl)^+$ (calcd m/z 593.10). Single crystals suitable for X-ray diffraction were obtained by recrystallisation in DCM and methanol solution.

[Ru(η^6-p-cymene)(Cl)(L3)] (6): Orange solid. Yield = 0.180 g (78%); M.p.: 196^{0}C (with decomposition); Calculated: $C_{33}H_{31}ClN_2O_2Ru$: C, 63.50; H, 5.01; N, 4.49 %. Found: C, 63.48; H, 5.01; N, 4.48%. IR (KBr, cm^{-1}):1527 $\nu_{(C=N-N=C)}$, 1474 $\nu_{(N=C-O)}$, 1393 $\nu_{(C-O)}$. UV–Vis (CH_3CN, λ_{max}/nm (ε_{max}/dm^3 mol^{-1} cm^{-1}): 418 (1576), 271 (7294), 238 (13,110). ^{1}H NMR (400 MHz, $CDCl_3$) δ (ppm): 9.59 (s, 1H, HC=N), 6.87-8.68 (m, 13H, aromatic), 5.35 (d, 1H, p-

cym-H), 5.34 (d, 1H, p-cym-H), 5.00 (d, 1H, p-cym-H), 4.36 (d, 1H, p-cym-H), 3.85 (s, 3H, OCH3), 2.48 (m, 1H, p-cym $CH(CH_3)_2$), 2.19 (s, 3H, p-cym CCH_3), 1.15 (d, 3H, p-cym $CH(CH_3)_2$, 0.99 (d, 3H, p-cym $CH(CH_3)_2$. ESI-MS: displays a peak at m/z 586.59 $(M - HCl)^+$ (calcd m/z 588.38).

X-ray crystallography

Single crystal of [Ru(η^6-p-cymene)(Cl)(L2)] (**5**) was grown by slow evaporation of dichloromethane-methanol solution at room temperature. A single crystal of suitable size was covered with Paratone oil, mounted on the top of a glass fiber, and transferred to a Bruker AXS Kappa APEX II single crystal X-ray diffractometer using monochromated MoKα radiation (λ=0.71073). Data were collected at 293K. The structure was solved with direct method using SIR-97 and was refined by full matrix least-squares method on F_2 with SHELXL-97.[26] Non-hydrogen atoms were refined with anisotropy thermal parameters. All hydrogen atoms were geometrically fixed and collected to refine using a riding model. Frame integration and data reduction were performed using the Bruker SAINT Plus (Version 7.06a) software. The multi scan absorption corrections were applied to the data using SADABS software. Figure 1 was drawn with ORTEP[27] and the structural data deposited at The Cambridge Crystallographic Data Centre: CCDC **1477541**.

Lipophilicity

The hydrophobicity values of the complexes **1-6** were measured by the "Shake flask" method in octanol - water phase partitions. Complexes **1-6** were dissolved in a mixture of water and *n*-octanol followed by shaking for 1 hour. The mixture was allowed to settle over a period of 30 minutes and the resulting two phases were collected separately without cross contamination of one solvent layer into another. The concentration of the complexes in each phase was determined by UV-Vis absorption spectroscopy at room temperature. The results are given as the mean values obtained from three independent experiments. The sample solution concentration was used to calculate log *P*. Partition coefficients for **1-6** were calculated using the equation log *P* = log[(**1-6**)oct/(**1-6**)aq].

Cell culture and inhibition of cell growth.

Cell culture. HeLa (human cervical cancer cell line), MDA-MB-231 (Triple negative breast carcinoma), Hep G2 (human liver carcinoma cell line) and NIH 3T3

(noncancerous cell, mouse embryonic fibroblast) were obtained from the National Centre for Cell Science (NCCS), Pune. These cell lines were cultured as a monolayer in RPMI-1640 medium (Biochrom AG, Berlin, Germany), supplemented with 10% fetal bovine serum (Sigma-Aldrich, St. Louis, MO, USA) and with 100 U mL^{-1} penicillin and 100 µg mL^{-1} streptomycin as antibiotics (Himedia, Mumbai, India), at 37 ^{o}C in a humidified atmosphere of 5% CO_2 in a CO_2 incubator (Heraeus, Hanau, Germany).

Inhibition of cell growth

The IC_{50} values, which are the concentrations of the tested compounds that inhibit 50% of cell growth, were determined using a 3–(4,5-dimethyl thiazol-2yl)-2,5-diphenyl tetrazolium bromide (MTT) assay. Cells were plated in their growth medium at a density of 5000 cells per well in 96 flat bottomed well plates. After 24 h plating, the Ru(II) arene benzhydrazone complexes **1-6** were added at different concentrations (1-100 µM for 24 h, with a final volume in the well of 250 µL) for 24 h to study the dose dependent cytotoxic effect. To each well, 20 µL of 5 mg mL^{-1} MTT in phosphate-buffer (PBS) was added. The plates were wrapped with aluminium foil and incubated for 4 h at 37 ˚C. The purple formazan product was dissolved by addition of 100 µL of 100% DMSO to each well. The quantity of formazan formed gave a measure of the number of viable cells. HeLa, MDA-MB-231 and Hep G2 were used for the MTT assay. The absorbance was monitored at 570 nm (measurement) and 630 nm (reference) using a 96 well plate reader (Bio-Rad, Hercules, CA, USA). Data were collected for four replicates each and used to calculate the respective means. The percentage of inhibition was calculated, from this data, using the formula: Percentage inhibition = 100 x {Mean OD of untreated cells (control) – Mean OD of treated cells} /{Mean OD of untreated cells (control)}. The IC_{50} value was determined as the complex concentration that is required to reduce the absorbance to half that of the control.

Acridine orange and ethidium bromide staining experiment

The changes in chromatin organization in MDA-MB-231 cells after treatment with IC_{50} concentration of the complexes **4** and **6** by using acridine orange (AO) and ethidium bromide (EB). 5 x 10^5 cells were allowed to adhere overnight on a coverslip placed in each well of a 12-well plate. The cells were allowed to recover for 1 h,

washed thrice with DPBS, stained with an AO and EB mixture (1:1, 10 μM) for 15 min, and observed with epifluorescence microscope (Carl Zeiss, Germany).

Hoechst 33258 staining method

Hoechst 33258 staining was done using the method described earlier with slight modifications. 5×10^5 MDA-MB-231 cells were treated with IC_{50} concentration of the complexes **4** and **6** for 24 h in a 6-well culture plate and were fixed with 4% paraformaldehyde followed by permeabilization with 0.1% Triton X-100. Cells were then stained with 50 μg mL^{-1} Hoechst 33258 for 30 min at room temperature. The cells undergoing apoptosis, represented by the morphological changes of apoptotic nuclei, were observed and imaged by epifluorescence microscope (Carl Zeiss, Germany).

Apoptosis evaluation - Flow cytometry

The MDA-MB-231 cells were grown in a 6-well culture plate and exposed to IC_{50} concentrations of complexes **4** and **6** for 24 h. The Annexin V-FITC kit uses annexin V conjugated with fluorescein isothiocyanate (FITC) to label phosphatidylserine sites on the membrane surface of apoptotic cells. Briefly the cells were trypsinised and washed with Annexin binding buffer and incubated with Annexin V-FITC and PI for 30 minutes and immediately analysed using flow cytometer FACS Aria-II. The results were analysed using DIVA software and percentage positive cells were calculated.

Cellular DNA damage by the comet assay

DNA damage was quantified by means of the comet assay as described. Assays were performed under red light at 4 ^oC. Cells used for the comet assay were sampled from a monolayer during the growing phase, 24 h after seeding. MDA-MB-231 cells were treated with the complexes **4** and **6** at IC_{50} concentration, and cells were harvested by a trypsinization process at 24 h. A total of 200 μL of 1% normal agarose in PBS at 65 ^oC was dropped gently onto a fully frosted microslide, covered immediately with a coverslip, and placed over a frozen ice pack for about 5 min. The coverslip was removed after the gel had set. The cell suspension from one fraction was mixed with 1% low-melting agarose at 37 ^oC in a 1:3 ratio. A total of 100 μL of this mixture was applied quickly on top of the gel, coated over the microslide, and allowed to set as before. A third coating of 100 μL of 1% low-melting agarose was placed on the gel

containing the cell suspension and allowed to set. Similarly, slides were prepared (in duplicate) for each cell fraction. After solidification of the agarose, the coverslips were removed, and the slides were immersed in an ice-cold lysis solution (2.5 M NaCl, 100 mM Na_2EDTA, 10 mM Tris, NaOH; pH 10, 0.1% Triton X-100) and placed in a refrigerator at 4 ^oC for 16 h. All of the above operations were performed in low-lighting conditions in order to avoid additional DNA damage. Slides, after removal from the lysis solution, were placed horizontally in an electrophoresis tank. The reservoirs were filled with an electrophoresis buffer (300 mM NaOH and 1 mM Na_2EDTA, pH > 13) until the slides were just immersed in it. The slides were allowed to stand in the buffer for about 20 min (to allow DNA unwinding), after which electrophoresis was carried out at 0.8 v cm^{-1} for 15 min. After electrophoresis, the slides were removed, washed thrice in a neutralization buffer (0.4 M Tris, pH 7.5), and gently dabbed to dry. Nuclear DNA was stained with 20 μL of EB (50 μg mL^{-1}). Photographs were taken using an epifluorescence microscope (Carl Zeiss).

Hemocompatibility assay

Fresh blood was collected from healthy volunteers in sterile lithium heparin vacutainers. Further, Red blood cells (RBCs) were separated by centrifugation (1500 rpm for 10 min at 4 °C) and a ficoll density gradient. After discarding the supernatant containing plasma and platelets, the RBCs were washed thrice with sterile phosphate buffered saline (PBS). Then, the pellets (1 ml) were resuspended in 3 ml of PBS. Then, 0.1 ml of the diluted RBC suspension was added to complexes **1-6** mixed in 0.5 ml PBS suspension at their respective IC_{50} concentration (24.12, 27.04, 14.23,18.94, 23.23, 13.78 μM) and incubated at 37 °C for 4 h. After incubation, all the samples were centrifuged at 12,000 rpm at 4 °C and supernatants were transferred to a 96-well plate. The hemolytic activity was determined by measuring the absorbance at 570 nm (Biorad microplate reader model 550, Japan). Control samples of 0% lysis (PBS buffer) and 100% lysis (in 1% Triton X-100) were employed in the experiment. The percent of hemolysis was calculated as follows:

$$\% \text{ Hemolysis} = (A_s - A_n)/ (A_p - A_n) \times 100\%$$

Where, A_s, A_n, and A_p are the absorbance of sample, negative control and positive control respectively.

Statistical Analysis

Values are given as the mean ± SD. Data are represented as averages of independent experiments, performed in duplicate or triplicate. Statistical analyses were done using the Student's *t* test. $P < 0.05$ was considered statistically significant.

Results and Discussion

The hydrazone ligand derivatives were conveniently prepared in an excellent yield by the condensation of 9-Anthraldehyde with substituted benzhydrazides in an equimolar ratio. These ligands were allowed to react with the ruthenium(II) arene precursor $[(\eta^6\text{-arene})RuCl_2]_2$ (arene-benzene or *p*-cymene) in a 2:1 molar ratio in the presence of triethylamine as the base and the new complexes of the general formula, $[(\eta^6\text{-arene})Ru(L)Cl]$ (arene-benzene or *p*-cymene; L-substituted 9-Anthraldehyde benzhydrazone derivatives) **(Scheme 1)** were obtained in high yields. The addition of triethylamine to the reaction mixture was used to remove a proton from the imidol oxygen and to facilitate the coordination of the imidolate oxygen to the ruthenium(II) ion. All the complexes are air-stable and highly soluble in most organic solvents. The analytical data of all the ruthenium(II) arene benzhydrazone complexes are in good agreement with the molecular formula proposed.

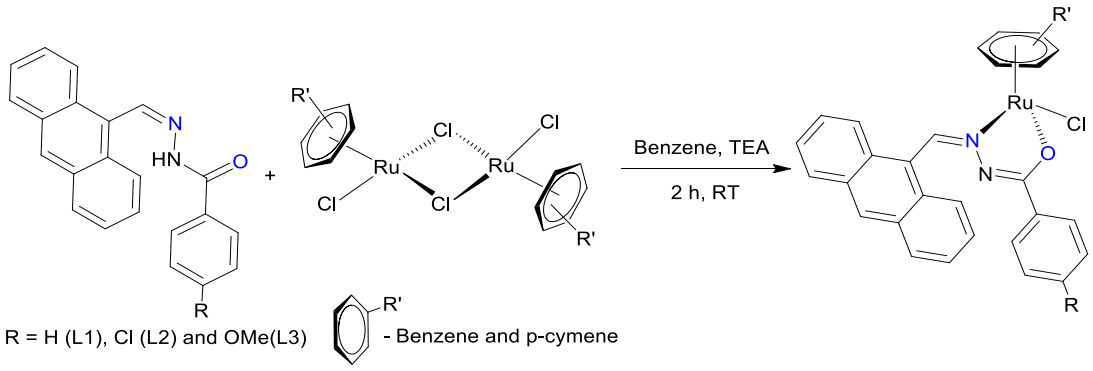

Scheme 1. Synthesis of Ru(II) arene benzhydrazone complexes.

Characterization of the complexes

The IR spectra of the free ligands displayed a medium to strong band in the region of 3180- 3196 cm^{-1} which is characteristic of the N-H functional group. The free ligands also displayed $\nu_{C=N}$ and $\nu_{C=O}$ absorptions in the region of 1548-1576 cm^{-1} and 1610-1653 cm^{-1} respectively, which indicate that the ligands exist in the amide form in the solid state. Bands that are due to ν_{N-H} and $\nu_{C=O}$ stretching vibrations were not observed with the complexes, which indicates that the ligands underwent tautomerization and subsequent coordination of

the imidolate enolate form during complexation. Coordination of the ligand to the ruthenium(II) ion through an azomethine nitrogen is expected to reduce the electron density in the azomethine link and thus lower the absorption frequency upon complexation 1527-1538 cm^{-1} which indicates the coordination of azomethine nitrogen to the ruthenium(II) ion. The band in the region of 1352-1393 cm^{-1} is due to the imidolate oxygen, which is coordinated to the metal. The IR spectra of all the complexes therefore confirm the mode of coordination of the benzhydrazone ligand to the ruthenium(II) ion *via* the azomethine nitrogen and imidolate oxygen.[28]

The absorption spectra of the ruthenium(II) arene benzhydrazone complexes in chloroform exhibited bands in the ultraviolet region below 278 nm are very similar and are attributable to the transitions within the ligand orbitals (n-π*, π-π*) taking place in the anthracene benzhydrazone ligands. The lowest energy absorption bands in the electronic spectra of the complexes in the visible region 409-421 nm are ascribed to MLCT (metal to ligand charge transfer) transitions. Based on the pattern of the electronic spectra of all the complexes an octahedral environment around the ruthenium(II) ion has been proposed similar to that of the other octahedral ruthenium(II) arene complexes.[29] The light emitting property of all the complexes was investigated in DMSO at ambient temperature (298 K). The excitation was made at the charge transfer band for all the complexes. The emission maxima of all the complexes have experienced a positive shift of the order of 90-98 nm. The emission maximum fall in the range 490-498 nm. It is likely that the emission originates from the lowest energy metal to ligand charge transfer (MLCT) state, probably derived from the excitation involving dπ(Ru) - π* (ligand), MLCT transitions, similar to the MLCT observed in other reported Ru(II) arene complexes. [29,30]

The ^{1}H NMR spectra of all the complexes were recorded in $CDCl_3$ to confirm the bonding of the benzoylhydrazone ligand to the ruthenium (II) ion. Multiplets observed in the region δ 6.87-8.68 ppm in the complexes have been assigned to the aromatic protons of benzhydrazone ligands. The signal due to the azomethine proton appears in the region δ 9.60-9.71 ppm. The position of the azomethine signal in the complexes is slightly downfield in comparison with that of the free ligand, suggesting deshielding of the azomethine proton due to its coordination to ruthenium. The singlet due to the -NH proton of the free ligand in the region δ 11.22-11.60 ppm is absent in the complex, further supporting enolisation and coordination of the imidolate oxygen to the Ru(II) ion. Therefore, the ^{1}H NMR spectra of the complexes confirm the bidentate coordination mode of the benzhydrazone ligands to ruthenium(II) ion. In all the complexes, the cymene protons are appeared in the region of δ

4.36-5.36 ppm.[31] In addition, the two isopropyl methyl protons of the p-cymene appeared as two doublet in the region of δ 0.98-1.51 ppm and the methine protons comes in the region of δ 2.43-2.48 ppm as septet. Further, the methyl group of the p-cymene comes as singlet around the region of δ 2.15-2.19 ppm. Additionally methoxy protons are observed as singlet for complexes **3** and **6** at δ 3.13-3.84 ppm. On the other hand, benzene arene protons displayed an upfield shift relative to complex **4**-**6** in the region δ 4.62-4.64 ppm. (Figure S1, Supporting Information).

The ESI-MS spectra of the complexes have been acquired to explain the relative composition and stability of the complexes. Thus, we have recorded mass spectra for all the complexes which confirm the formation of the complexes. Mass spectrometric measurements carried out under positive ion ESI mode using acetonitrile as the solvent. In their positive ESI mass spectra **1**-**6** showed major peaks due to cationic fragment $[(\eta^6\text{-arene})Ru(L)Cl]^+$ generated by loss of the Cl^-. The ESI spectra of complexes **1**-**6** display peaks at m/z 502.46 (**1**, M - Cl)$^+$, 537.02 (**2**, M - Cl)$^+$, 532.58 (**3**, M - Cl)$^+$, 559.05 (**4**, M - Cl)$^+$, 591.75 (**5**, M - Cl - H)$^+$ and 586.59 (**6**, M - Cl - H)$^+$ respectively. The mass spectrometry results are in good agreement with the proposed molecular formulae of the complexes and suggest that chloro (Cl^-) group is labile and possibly replaced by targeted biomolecules.

X-ray crystallographic studies

Attempts were made to grow single crystals for all the complexes to confirm the coordination mode of the ligand to metal and geometry of the complex. Molecular structure of [Ru(η^6-p-cymene)(Cl)(L5)] (**5**) have been determined by single-crystal X-ray diffraction analyses. Crystal of **5** grew from slow diffusion of dichloromethane into methanol solutions and crystallized in the triclinic system with $P\bar{1}$ space group. The selected bond lengths and bond angles are given in Table 2 whereas crystallographic data and structural refinement parameters are gathered in Table 1. The ORTEP views of the molecules with the atom numbering are shown in Figure 3. The molecular structure of the complex **5** shows clearly that the benzhydrazone ligand coordinates in a bidentate manner to ruthenium ion *via* the azomethine nitrogen and imidolate oxygen in addition to one chlorine and one arene group. The complex adopts the commonly observed piano-stool geometry as reported in many half-sandwich arene ruthenium(II) complexes.[32] In this case, the arene ring forms the seat of the piano-stool, while the bidentate benzhydrazone N, O and Cl ligands form the three legs of the stool. Therefore, ruthenium(II) ion is sitting in a NOCl (η^6-arene) coordination environment.

The benzhydrazone ligand bind to the metal centre at N and O forming the five membered chelate ring with bite angle 75.94(9)^{o} O(1)-Ru(1)-N(2) and 83.25(8)^{o} N(2)-Ru(1)-Cl(1). The bond lengths of Ru(1)-N(2) and Ru(1)-O(1) are 2.105(3) Å and 2.056(2) Å respectively. The Ru-Cl bond length is found to be 2.4105(13) Å and the bond length is in agreement with other structurally characterized *p*-cymene ruthenium complexes.[33] The ruthenium atom is π bonded to the arene ring with an average Ru-C distance of 2.173(3) Å, whereas average C-C bond length in the arene ring is 1.482(4) Å with alternating short and long bonds. As all the complexes display similar spectral properties, the other five complexes are assumed to have similar structure to that of [Ru(η^6-p-cymene)(Cl)(L2)] (**5**).

Table 1. Selected crystal data and structure refinement summary of **5**.

Complex	**5**
Chemical formula	C_{32} H_{28} Cl_2 N_2 O Ru
Formula weight	628.53
Temperature	296(2) K
Crystal system	Triclinic
Space group	$P\overline{1}$
a (Å)	9.951 (2)
b (Å)	11.437 (2)
c (Å)	13.867 (3)
α (°)	69.55 (3)
β (°)	71.55 (3)
γ (°)	73.82 (3)
Volume (Å^3)	1377.4 (5)
Z	2
ρ (Mg/m^3)	1.515
μ (mm^{-1})	0.792
Reflections collected	21062
Final R indices [I>2σ(I)]	R_1 = 0.0319, wR_2 = 0.0911
R indices (all data)	R_1 = 0.0370, wR_2 = 0.1035
Goodness-of-fit on F^2	1.152

Table 2. Selected Bond Lengths (Å) and Angles (deg) in **5**

distances/angles	**5**
Ru(1)-N(2)	2.105(3)
Ru(1)-O(1)	2.056(2)
Ru(1)-Cl(1)	2.4105(13)
Ru(1)-C(10)	2.173(3)
N(1)-N(2)	1.400(3)
N(2)-C(18)	1.283(4)
O(1)-C(1)	1.292(4)
O(1)-Ru(1)-N(2)	75.94(9)
N(2)-Ru(1)-Cl(1)	83.25(8)
N(2)-N(1)-Ru(1)	114.48(18)
C(1)-O(1)-Ru(1)	112.89(18)
C(1)-N(2)-N(1)	110.5(2)
C(13)-Ru(1)-Cl(1)	92.62(11)
O(1)-Ru(1)-Cl(1)	84.36(7)

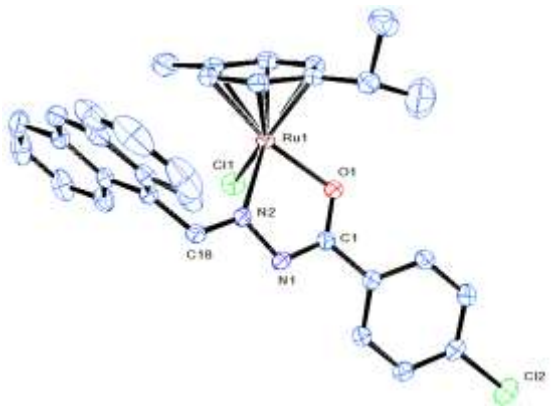

Figure 3. ORTEP drawing of complex **5** at 30% probability level, with hydrogen atoms being omitted for clarity. The solvent molecule has been omitted for clarity.

Lipophilicity

The hydrophobicity of metal complexes is an important parameter to determine the penetration behaviour across the cell membrane, and is investigated in terms of the partition coefficient (log P). Here, the complexes are likely to differ in their hydrophobicity due to the variation in the different substitutions present in the complexes. These measurements are based on solubility of a given compound in an aqueous vs organic medium. Based on the concentration of a given compound distributed in the biphasic system (n-octanol–water).[34] The calculated log *P* values for complexes **1-6** are 2.49, 2.55, 2.36, 2.18, 2.23 and 1.82

respectively (Table 2). Among the all complexes, complexes having p-cymene with methoxy substituent (**6)** shows higher hydrophobicity than other rest of the complexes (**1-5**).

***In Vitro* antiproliferative activity**

All the ruthenium complexes **1-6** and the free benzhydrazone ligands evaluated for their cytotoxic activity against HeLa, MDA-MB-231 and Hep-G2 along with NIH 3T3 cell lines by using the MTT [3-(4,5-dimethylthiazol-2-yl)-2,5-diphenyltetrazolium bromide] assay (colorimetric assay) that measures mitochondrial dehydrogenase activity as an indication of cell viability. Because these complexes might undergo ligand substitution reactions with water molecules when dissolved in aqueous solutions, freshly made stock solutions of each compound were used. The widely used clinical drug, cisplatin, was included as a positive control. The effects of the ruthenium(II) arene complexes to arrest the proliferation of cancer cells were investigated after an exposure of 24 h. It is to be noted that the ligands did not show any inhibition of the cell growth even up to 100 μM and clearly indicates chelation of the benzoylhydrazone ligand with metal ion is responsible for the observed cytotoxicity properties of the complexes. The results of MTT assays revealed that complexes showed notable activity against the cell lines HeLa, MDA-MB-231 and Hep-G2 with respect to IC_{50} values (Table 2). From the IC_{50} values obtained it was inferred that complex **6** are highly active against all the cell lines with very low IC_{50} values than that of the well-known anticancer drug cisplatin. In addition, the *in vitro* cytotoxic activity studies of the complexes against the mouse embryonic fibroblast cell line NIH 3T3 (normal cells) was undertaken and the IC_{50} values are above 229 μM, which confirmed that the complexes are very specific on cancer cells. These ruthenium(II) arene benzhydrazone complexes **1-6** posses significant cytotoxicity over the ligands may be due to the presence of extended π conjugation resulting from the chelation of Ru(II) ion with the ligand. Further, the observed higher activity of the complexes **4** and **6** is correlated to the nature of the chelating benzoylhydrazone ligand and arene moiety.

Further, the observed cytotoxic activity of complexes **3** and **6** were found to be superior when compared with other complexes. The observed higher efficiency of complexes **3** and **6** are related to the nature of the substitution of the benzhydrazone ligand that is coordinated to the ruthenium ion. Higher cytotoxicity is observed for complexes **3** and **6**, which contains an electron-donating methoxy group that consequently increases the lipophilic character of the metal complex, which favours its permeation through the lipid layer of a cell

membrane. Apart from the three different cell lines, the proliferation of the MDA-MB-231 cell line was arrested to a greater extent than that of HeLa and Hep-G2 cells by the complexes.[35]

On the other hand, the arene group also imparts hydrophobic character to the molecule, which facilitates the passive diffusion through the cell membrane, enhancing the cellular accumulation on the antitumor activity of these ruthenium complexes. It has been observed that complexes **4-6** with a p-cymene group show higher potency than those with a benzene group in complex **3**, which may be attributed to the stronger hydrophobic interactions between the Ru (II)-cymene complex and the biomolecular targets.[36] Complex **6** shows high cytotoxic activity with very low IC_{50} values of 11.40 ± 0.7, 4.13 ± 0.4 and 9.19 ± 0.3 μM toward HeLa, MDA-MB-231 and Hep-G2. Further, the IC_{50} values are much lower than those previously reported for other Ru(II) arene arylazo, 2-thiosalicylic acid, phenanthroimidazole or polypyridyl complexes.[37]

Table 2. Cytotoxicity (IC_{50}, μM) of ligand and complexes **1-6**. (n.e.: no effect) and calculated partition coefficients (log *P*).

Complex	IC_{50} values (μM)				log *P*
	HeLa	MDA-MB-231	Hep G2	NIH3T3	
Complex **1**	24.12 ± 0.1	19.41 ± 0.3	21.32 ± 0.2	232.13 ± 0.5	2.49 ± 0.3
Complex **2**	27.04 ± 0.2	23.01 ± 0.1	26.49 ± 0.3	241.47 ± 0.6	2.55 ± 0.5
Complex **3**	14.23 ± 0.4	11.29 ± 0.4	13.57 ± 0.1	248.51 ± 0.3	2.36 ± 0.4
Complex **4**	18.94 ± 0.3	9.97 ± 0.2	11.86 ± 0.2	239.12 ± 0.4	2.18 ± 0.4
Complex **5**	23.23 ± 0.1	18.03 ± 0.3	23.06 ± 0.2	229.79 ± 0.5	2.23 ± 0.5
Complex **6**	13.78 ± 0.1	5.03 ± 0.2	10.18 ± 0.3	243.81 ± 0.5	1.82 ± 0.4
L1	n.e.	n.e.	n.e.	n.e.	
L2	n.e.	n.e.	n.e.	n.e.	
L3	n.e.	97.10 ± 0.3	99.12 ± 0.4	n.e.	
Cisplatin	21.32 ± 0.2	11.91 ± 0.6	19.16 ± 1.2	245.13 ± 0.4	

AO-EB and Hoechst staining assays

In order to observe the morphological changes, MDA-MB-231 cells were stained with acridine orange (AO) and ethidium bromide (EB). Since AO is a crucial dye that stains nuclear DNA across an intact cell membrane and EB only stains cells that have lost

membrane integrity. The living cells will be uniformly stained green, apoptotic cells are stained green and contain apoptotic characteristics such as cell blebbing, nuclear shrinkage and chromatin condensation, necrotic cells are stained as red and can be found by the AO-EB double staining. After MDA-MB-231 cells were exposed to complexes **4** and **6** for 24 h at IC_{50} concentration 24 h, the morphological changes are shown in Figure 4. In the control, the living cells of MDA-MB-231 were stained bright green in spots. The treatment of MDA-MB-231 cells with complexes **4** and **6**, green apoptotic cells with apoptotic characteristics such as nuclear shrinkage and chromatin condensation, as well as red necrotic cells, were observed. These observations indicate that complexes **4** and **6** can induce apoptosis in MDA-MB-231 cells.[38] Additionally complexes **4** and **6** treated MDA-MB-231 cells were stained with Hoechst 33258, apoptotic features such as nuclear shrinkage and chromatin condensation were also observed (Figure 5). Hence the results of AO-EB and Hoechst staining assays suggest that complexes **4** and **6** induce apoptosis in MDA-MB-231 cells.[39]

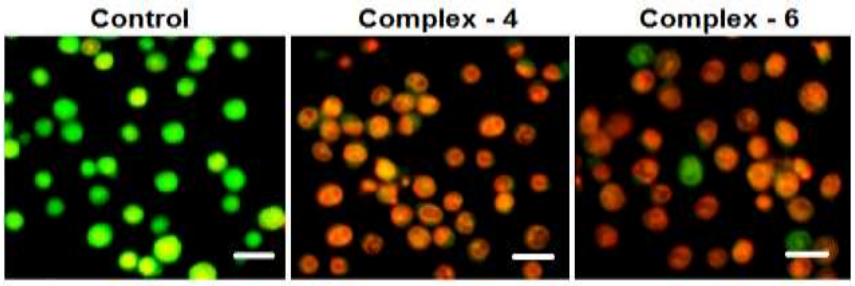

Figure 4. Morphological assessment of AO and EB of MDA-MB-231 cells treated with complexes **4** and **6** (IC_{50} concentration) for 24 h. The scale bar 20 µm.

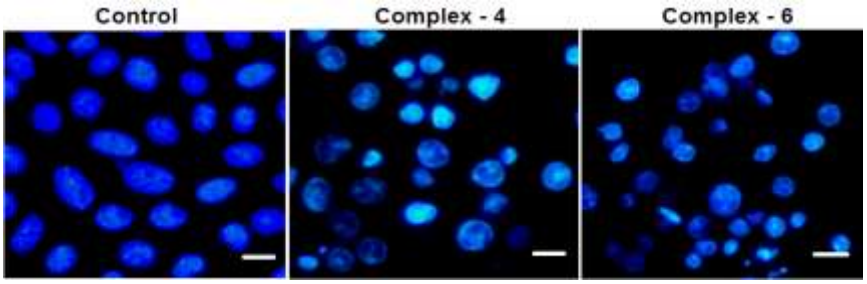

Figure 5. Morphological assessment of complexes **4** and **6** (IC_{50} concentration) and MDA-MB-231 cells for 24 h. The scale bar 20 µm.

Evaluation of apoptosis - Flow cytometry

The potential to induce apoptosis in cancer cells by the addition of synthesized complexes can be quantitatively investigated by flow cytometry analysis by Annexin V protocol, with the help of Annexin V-FITC Apoptosis Detection Kit to perform double-

staining with propidium iodide and Annexin V-FITC. Annexin V, a Ca^{2+} dependent phospholipid-binding protein with a high affinity for the membarane phospholipid phosphatidylserine (PS), is quite helpful for identifying apoptotic cells with exposed PS. Propidium iodide is a standard flow cytometric viability probe used to distinguish viable from non-viable cells (Figure 6). The MDA-MB-231 cells were treated with the complexes **4** and **6** at IC_{50} concentrations for 24 h. The cell death induced by the complexes follow a pathway from lower left quadrant to the upper right quadrant (Annexin V^+/PI^+) which represents cells undergoing apoptosis.[40]

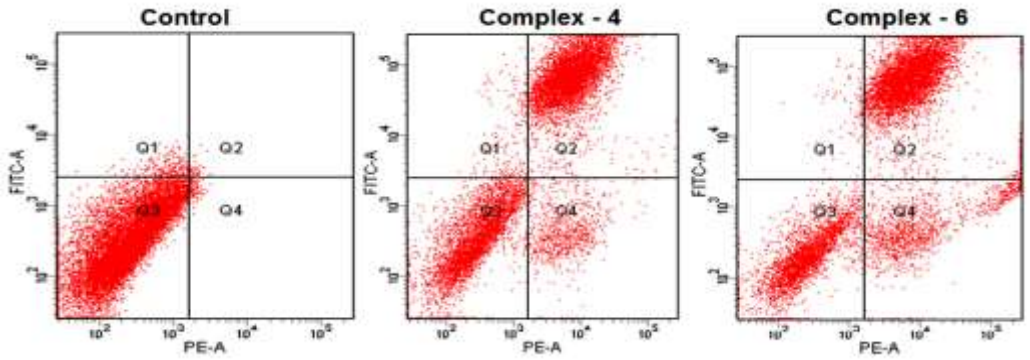

Figure 6. AnnexinV/propidium iodide assay of MDA-MB-231 cells treated by complexes **4** and **6** (IC_{50} concentration) measured by flow cytometry.

Comet assay

As is well known, DNA is considered as the target of most of the current antitumor drugs to conquer tumor. DNA fragment is the hallmark of apoptosis. The single cell gel electrophoresis assay (comet assay) is commonly utilized to assess DNA integrity. As shown in Figure 7, in control, MDA-MB-231 cells fail to show a comet like appearance. MDA-MB-231 cells were treated IC_{50} concentration of the complexes **4** and **6** 24 h, a statistically significant and well-formed comet was observed. The length of the comet tail is the symbol of the extent of DNA damage. With the IC_{50} concentration of the complexes, comet tails become more and more obvious. The results show that ruthenium(II) arene complexes are capable of eliciting DNA damaging effects, as evidenced by the comet assays on MDA-MB-231 cells. It is well known that DNA fragmentation is a hallmark of apoptosis.[41]

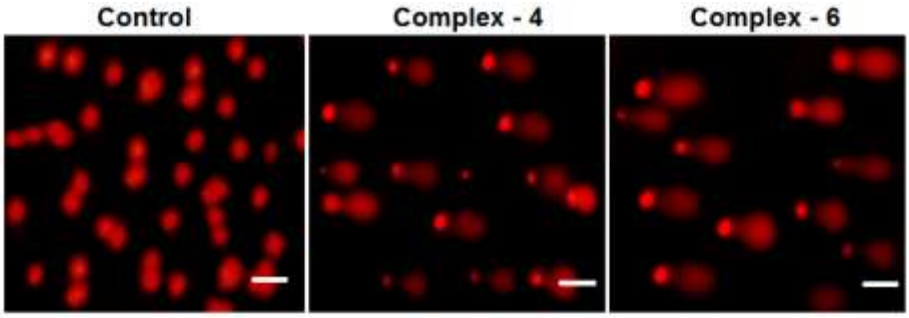

Figure 7. Comet assay of staining of EB control (untreated) MDA-MB-231 cells treated with complexes **4** and **6** (IC_{50} concentration) for 24 h. The scale bar 40 µm.

Hemocompatibility assay

Interaction of the drug with the blood components particularly human RBCs is an important and inevitable phenomenon, thus assessing the haemolysis becomes crucial in evaluating the blood compatibility of drugs. The result shows that complexes **1-6** show good compatibility with human RBCs. The mechanism of direct hemolytic activity for different toxic agents was found to be nonspecific. According to the International Organization for Standardization/Technical Report 7406, the admissible level of hemolysis of biological materials is 5%. As shown in Figure 8, compared to positive control (Triton X-100), all the complexes have exhibited negligible red hemoglobin release, implying that it is negligibly toxic or safe to normal cells.[42]

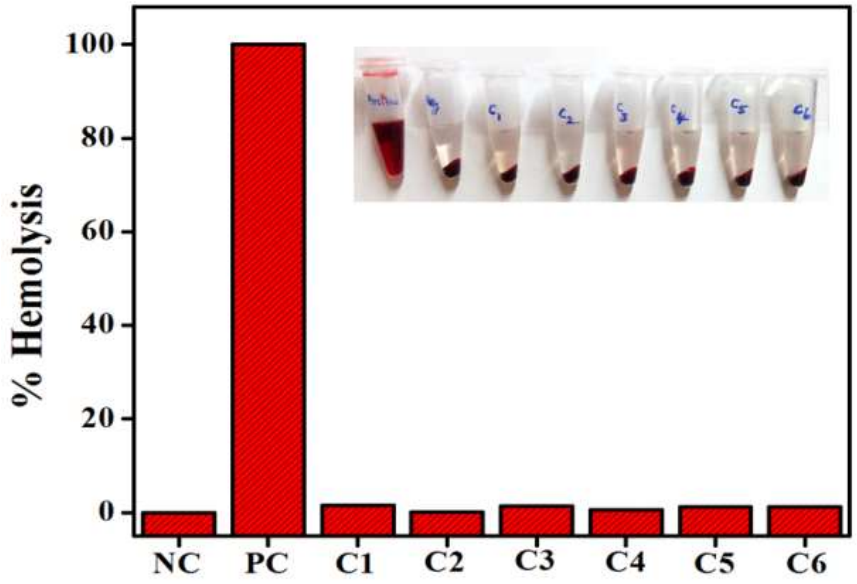

Figure 8. Human blood compatibility analysis of complexes **1-6**.

Conclusions

We report here the synthesis of six new ruthenium(II) arene complexes containing bidendate O and N chelating 9-anthraldehyde benzhydrazone ligands. All the complexes (**1-6)** have been fully characterized by analytical and spectral methods (IR, UV−vis, emission, ^{1}H NMR and ESI-MS). Molecular structure by X-ray diffraction study reveals that the benzhydrazone ligand coordinated to ruthenium *via* azomethine nitrogen and imidolate oxygen and adopts the familiar pseudo-octahedral "piano-stool" geometry. Interestingly, the cytotoxic activities of complex 6 against the tested cancer cell lines were significantly superior to that of the well-known anticancer drug cisplatin. Further, fluorescence staining techniques and flow cytometry using the annexin-V assay revealed that complexes **4** and **6** induce apoptosis in MDA-MB-231 cancer cells. Alkaline comet assay confirms the single-strand break of DNA. Hemolysis assays revealed that all the complexes **1-6** were less toxic to human RBCs. On the basis of the results, we suggest that ruthenium-arene based benzhydrazone complexes are attractive agents for development of future anticancer therapies relying on the combination of chemopreventive and chemotherapeutic agents for human cancers.

Acknowledgements

M. M. S. Khan thank the University Grants Commission (UGC), New Delhi for financial assistance through the UGC-BSR fellowship (Ref. No. F.7−22/2007(BSR)). We thank Dr. Yu Liu for crystallographic discussion. We express sincere thanks to DST-FIST, India for the use of Bruker 400 MHz spectrometer at the School of Chemistry, Bharathidasan University, Tiruchirappalli-24.

References

1. (a) L. Kelland, *Nat Rev Cancer*, 2007, **7**, 573-584; (b) J. M. Rademaker-Lakhai, D. van den Bongard, D. Pluim, J. H. Beijnen and J. H. M. Schellens, *Clinical Cancer Research*, 2004, **10**, 3717-3727; (c) S. Leijen, S. A. Burgers, P. Baas, D. Pluim, M. Tibben, E. Werkhoven, E. Alessio, G. Sava, J. H. Beijnen and J. H. M. Schellens, *Investigational New Drugs*, 2014, **33**, 201-214; (d) A. Bergamo, C. Gaiddon, J. H. M. Schellens, J. H. Beijnen and G. Sava, *Journal of Inorganic Biochemistry*, 2012, **106**, 90-99.

2. (a) M. Ohmichi, J. Hayakawa, K. Tasaka, H. Kurachi and Y. Murata, *Trends in Pharmacological Sciences*, 2005, **26**, 113-116; (b) S. L. Cooke and J. D. Brenton, *The Lancet Oncology*, 12, 1169-1174; (c) D. Wang and S. J. Lippard, *Nat Rev Drug Discov*, 2005, **4**, 307-320.

3. Giaccone, G. *Drugs*, 2000, **59**, 9 -17.

4. J. M. Rademaker-Lakhai, D. van den Bongard, D. Pluim, J. H. Beijnen and J. H. M. Schellens, *Clinical Cancer Research*, 2004, **10**, 3717-3727.

5. C. G. Hartinger, M. A. Jakupec, S. Zorbas-Seifried, M. Groessl, A. Egger, W. Berger, H. Zorbas, P. J. Dyson and B. K. Keppler, *Chemistry & Biodiversity*, 2008, **5**, 2140-2155.

6. M. Kubanik, H. Holtkamp, T. Söhnel, S. M. F. Jamieson and C. G. Hartinger, *Organometallics*, 2015, **34**, 5658-5668.

7. B. S. Murray, M. V. Babak, C. G. Hartinger and P. J. Dyson, *Coordination Chemistry Reviews*, 2016, **306**, Part 1, 86-114.

8. A. L. Noffke, A. Habtemariam, A. M. Pizarro and P. J. Sadler, *Chemical Communications*, 2012, **48**, 5219-5246.

9. (a) C. G. Hartinger, N. Metzler-Nolte and P. J. Dyson, Organometallics, 2012, 31, 5677-5685; (b) A. F. A. Peacock and P. J. Sadler, *Chemistry – An Asian Journal*, 2008, **3**, 1890-1899.

10. A. Grozav, O. Balacescu, L. Balacescu, T. Cheminel, I. Berindan-Neagoe and B. Therrien, *Journal of Medicinal Chemistry*, 2015, 58, 8475-8490.

11. Y. Geldmacher, R. Rubbiani, P. Wefelmeier, A. Prokop, I. Ott and W. S. Sheldrick, *Journal of Organometallic Chemistry*, 2011, 696, 1023-1031.

12. A. Kurzwernhart, W. Kandioller, S. Bächler, C. Bartel, S. Martic, M. Buczkowska, G. Mühlgassner, M. A. Jakupec, H.-B. Kraatz, P. J. Bednarski, V. B. Arion, D. Marko, B. K. Keppler and C. G. Hartinger, *Journal of Medicinal Chemistry*, 2012, **55**, 10512-10522.

13. W. Su, Q. Qian, P. Li, X. Lei, Q. Xiao, S. Huang, C. Huang and J. Cui, *Inorganic Chemistry*, 2013, **52**, 12440-12449.

14. R. Pettinari, C. Pettinari, F. Marchetti, B. W. Skelton, A. H. White, L. Bonfili, M. Cuccioloni, M. Mozzicafreddo, V. Cecarini, M. Angeletti, M. Nabissi and A. M. Eleuteri, *Journal of Medicinal Chemistry*, 2014, **57**, 4532-4542.

15. C. M. Clavel, E. Păunescu, P. Nowak-Sliwinska, A. W. Griffioen, R. Scopelliti and P. J. Dyson, *Journal of Medicinal Chemistry*, 2015, **58**, 3356-3365.

16. (a) T. Nasr, S. Bondock and M. Youns, *European Journal of Medicinal Chemistry*, 2014, **76**, 539-548; (b) T. Giraldi, P. M. Goddard, C. Nisi and F. Sigon, *Journal of Pharmaceutical Sciences*, 1980, **69**, 97-98.

17. R. Fernandez, M. Melchart, A. Habtemariam, S. Parsons, P.J. Sadler, *Chem. Eur. J*. 2004, **10**, 5173.

18. M. Frik, A. Martínez, B. T. Elie, O. Gonzalo, D. Ramírez de Mingo, M. Sanaú, R.S.Delgado, T. Sadhukha, S. Prabha, Joe W. Ramos, I. Marzo, and M. Contel, *J. Med. Chem*., 2014, **57**, 9995.

19. (a) T. P. Wunz, R. T. Dorr, D. S. Alberts, C. L. Tunget, J. Einspahr, S. Milton and W. A. Remers, *Journal of Medicinal Chemistry*, 1987, **30**, 1313-1321; (b) H. N. Kim, J. Lim, H. N. Lee, J.-W. Ryu, M. J. Kim, J. Lee, D.-U. Lee, Y. Kim, S.-J. Kim, K. D. Lee, H.-S. Lee and J. Yoon, *Organic Letters*, 2011, **13**, 1314-1317; (c) R. F. Pittillo and C. Woolley, Applied and Environmental Microbiology, **18**, 519−521.

20. J. Yellol, S. A. Pérez, A. Buceta, G. Yellol, A. Donaire, P. Szumlas, P. J. Bednarski, G. Makhloufi, C. Janiak, A. Espinosa and J. Ruiz,*J. Med. Chem.*, 2015, **58**, 7310.

21. A. Romero, T. Caldés, E. Díaz-Rubio and M. Martín, *Clinical and Translational Oncology*, 2012, 14, 163-168.

22. (a) M. Varache-Lembège, S. Moreau, S. Larrouture, D. Montaudon, J. Robert and A. Nuhrich, *European Journal of Medicinal Chemistry*, 2008, **43**, 1336-1343; (b) H. A. Abdel-Aziz, T. Aboul-Fadl, A.-R. M. Al-Obaid, M. Ghazzali, A. Al-Dhfyan and A. Contini, *Archives of Pharmacal Research*, 2012, **35**, 1543-1552.

23. (a) M. Alagesan, P. Sathyadevi, P. Krishnamoorthy, N. S. P. Bhuvanesh and N. Dharmaraj, *Dalton Transactions*, 2014, **43**, 15829-15840; (b) E. Singleton and H. E. Swanepoel, *Inorg Chim Acta*, 1982, **57**, 217-221.

24. (a) M. A. Bennett and A. K. Smith, *J. Chem. Soc., Dalton Transactions*, 1974, 233-241; (b) M. A. Bennett, T. N. Huang, T. W. Matheson, A. K. Smith, S. Ittel and W. Nickerson, *Inorganic Synthesis*, 1982, 74-78.

25. S. Mondal, C. Das, B. Ghosh, B. Pakhira, A. J. Blake, M. G. B. Drew and S. K. Chattopadhyay, *Polyhedron*, 2014, 80, 272-281.

26. G. Sheldrick, *Acta Crystallographica Section A*, 2008, **64**, 112-122.

27. L. Farrugia, *Journal of Applied Crystallography*, 1997, **30**, 565.

28. (a) R. J. Butcher, J. Jasinski, G. M. Mockler and E. Sinn, *Journal of the Chemical Society, Dalton Transactions*, 1976, 1099-1102; (b) R. N. Prabhu and R. Ramesh, *RSC Advances*, 2012, **2**, 4515-4524.

29. K. N. Kumar, G. Venkatachalam, R. Ramesh and Y. Liu, *Polyhedron*, 2008, **27**, 157-166.

30. (a) A. Juris, L. Prodi, A. Harriman, R. Ziessel, M. Hissler, A. El-ghayoury, F. Wu, E. C. Riesgo and R. P. Thummel, *Inorganic Chemistry*, 2000, **39**, 3590-3598; (b) J. V. Ortega, K. Khin, W. E. van der Veer, J. Ziller and B. Hong, *Inorganic Chemistry*, 2000, **39**, 6038-6050; (c) R. N. Prabhu, D. Pandiarajan and R. Ramesh, *Journal of Organometallic Chemistry*, 2009, 694, 4170-4177.

31. (a) M. U. Raja and R. Ramesh, *Journal of Organometallic Chemistry*, 2012, **699**, 5-11; (b) M. Kalidasan, R. Nagarajaprakash, S. Forbes, Y. Mozharivskyj and K. M. Rao, *Zeitschrift für anorganische und allgemeine Chemie*, 2015, **641**, 715-723.

32. F. Marchetti, C. Pettinari, R. Pettinari, A. Cerquetella, C. Di Nicola, A. Macchioni, D. Zuccaccia, M. Monari and F. Piccinelli, *Inorganic Chemistry*, 2008, **47**, 11593-11603; (b) (b) D. Pandiarajan and R. Ramesh, *Journal of Organometallic Chemistry*, 2013**, 723**, 26-35.

33. (a) J. Valladolid, C. Hortiguela, N. Busto, G. Espino, A. M. Rodriguez, J. M. Leal, F. A. Jalon, B. R. Manzano, A. Carbayo and B. Garcia, *Dalton Transactions*, 2014, **43**, 2629-2645; (b) R. Pettinari, C. Pettinari, F. Marchetti, B. W. Skelton, A. H. White, L. Bonfili, M. Cuccioloni, M. Mozzicafreddo, V. Cecarini, M. Angeletti, M. Nabissi and A. M. Eleuteri, *Journal of Medicinal Chemistry*, 2014, **57**, 4532-4542.

34. (a) V. Vajpayee, Y. J. Yang, S. C. Kang, H. Kim, I. S. Kim, M. Wang, P. J. Stang and K.-W. Chi, *Chemical communications (Cambridge, England)*, 2011, **47**, 5184-5186; (b) M. Kubanik, H. Holtkamp, T. Söhnel, S. M. F. Jamieson and C. G. Hartinger, *Organometallics*, 2015, **34**, 5658-5668; (c) R. K. Gupta, G. Sharma, R. Pandey, A. Kumar, B. Koch, P.-Z. Li, Q. Xu and D. S. Pandey, *Inorganic Chemistry*, 2013, **52**, 13984-13996; (d) S. Mukhopadhyay, R. K. Gupta, R. P. Paitandi, N. K. Rana, G. Sharma, B. Koch, L. K. Rana, M. S. Hundal and D. S. Pandey, *Organometallics*, 2015, **34**, 4491-4506.

35. (a) A. Habtemariam, M. Melchart, R. Fernández, S. Parsons, I. D. H. Oswald, A. Parkin, F. P. A. Fabbiani, J. E. Davidson, A. Dawson, R. E. Aird, D. I. Jodrell and P. J. Sadler, *Journal of Medicinal Chemistry*, 2006, **49**, 6858-6868; (b) R. E. Morris, R. E. Aird, P. del Socorro Murdoch, H. Chen, J. Cummings, N. D. Hughes, S. Parsons, A. Parkin, G. Boyd, D. I. Jodrell and P. J. Sadler, *Journal of Medicinal Chemistry*, 2001, **44**, 3616-3621.

36. (a) É. A. Enyedy, G. M. Bognár, T. Kiss, M. Hanif and C. G. Hartinger, *Journal of Organometallic Chemistry*, 2013, 734, 38-44; (b) J. Ruiz, V. Rodríguez, N. Cutillas, A. Espinosa and M. J. Hannon, *Inorganic Chemistry*, 2011, **50**, 9164-9171.

37. (a) L. He, S.-Y. Liao, C.-P. Tan, R.-R. Ye, Y.-W. Xu, M. Zhao, L.-N. Ji and Z.-W. Mao, *Chem. Eur. J.* 2013, **19**, 12152-12160; (b) Q. Wu, C. Fan, T. Chen, C. Liu, W. Mei, S. Chen,

B. Wang, Y. Chen and W. Zheng, *European Journal of Medicinal Chemistry*, 2013, **63**, 57-63; (c) R. Pettinari, C. Pettinari, F. Marchetti, B. W. Skelton, A. H. White, L. Bonfili, M. Cuccioloni, M. Mozzicafreddo, V. Cecarini, M. Angeletti, M. Nabissi and A. M. Eleuteri, *Journal of Medicinal Chemistry*, 2014, **57**, 4532-4542; (d) Q. Wu, K. Zheng, S. Liao, Y. Ding, Y. Li and W. Mei, *Organometallics*, 2016, **35**, 317-326; (e) M. Hanif, S. Meier, A. Nazarov, J. Risse, A. Legin, A. Casini, M. A. Jakupec, B. K. Keppler and C. G. Hartinger, *Frontiers in Chemistry*, 2013, 1-7.

38. R. K. Gupta, R. Pandey, G. Sharma, R. Prasad, B. Koch, S. Srikrishna, P.-Z. Li, Q. Xu and D. S. Pandey, *Inorganic Chemistry*, 2013, **52**, 3687-3698.

39. (a) Z.-F. Chen, Q.-P. Qin, J.-L. Qin, Y.-C. Liu, K.-B. Huang, Y.-L. Li, T. Meng, G.-H. Zhang, Y. Peng, X.-J. Luo and H. Liang, *Journal of Medicinal Chemistry,* 2015, **58**, 2159-2179.

40. (a) J. P. Johnpeter, G. Gupta, J. M. Kumar, G. Srinivas, N. Nagesh and B. Therrien, *Inorganic Chemistry*, 2013, **52**, 13663-13673; (b) B. Banik, K. Somyajit, G. Nagaraju and A. R. Chakravarty, *Dalton Transactions*, 2014, **43**, 13358-13369.

41. R. M. Lord, A. J. Hebden, C. M. Pask, I. R. Henderson, S. J. Allison, S. L. Shepherd, R. M. Phillips and P. C. McGowan, *Journal of Medicinal Chemistry*, 2015, **58**, 4940-4953.

42. (a) H.-W. An, S.-L. Qiao, C.-Y. Hou, Y.-X. Lin, L.-L. Li, H.-Y. Xie, Y. Wang, L. Wang and H. Wang, *Chemistry Communications*, 2015, **51**, 13488–13491; (b) B. Naeye, H. Deschout, M. Roding, M. Rudemo, J. Delanghe, K. Devreese, J. Demeester, K. Braeckmans, S. C. De Smedt and K. Raemdonck, *Biomaterials*, 2011, **32**, 9120–9127; (c) K. Purkait, S. Chatterjee, S. Karmakar and A. Mukherjee, *Dalton Transactions*, 2016, **45**, 8541-8555.